Bulletin of Applied Mathematics and Mathematics Education
Volume 2, Number 2, October 2022 pp. 65-78
https://dx.doi.org/10.12928/bamme.v2i2.7617
e-ISSN 2776-1029, p-ISSN 2776-1002

Optimal control on education, vaccination, and treatment in the model of dengue hemorrhagic fever

Eva Annisa Haafidhoh[1*], Yudi Ari Adi[1], Nursyiva Irsalinda[1,2]

[1]Department of Mathematics, Universitas Ahmad Dahlan, Jl. Jend. Ahmad Yani, Tamanan, Banguntapan, Bantul, DIY 55191 Indonesia
[2]Department of Mathematics, Universiti Malaysia Terengganu, 21030 Kuala Nerus, Terengganu, Malaysia

*Corresponding e-mail: eva1800015073@webmail.uad.ac.id

ARTICLE INFO

Article History
Received 21 July 2022
Revised 25 October 2022
Accepted 5 December 2022

Keywords
SEIR epidemic model,
Dengue hemorrhagic fever,
Optimal control,
Pontryagin minimum principle.

How to cite this article:
Haafidhoh, E. A., Adi, Y. A., & Irsalinda, N. (2022). Optimal control on education, vaccination, and treatment in the model of dengue hemorrhagic fever. *Bulletin of Applied Mathematics and Mathematics Education*, *2*(2), 65-78.

ABSTRACT

Dengue hemorrhagic fever (DHF) is an infection caused by the dengue virus which is transmitted by the Aedes aegypti mosquito. In this paper, a model of the spread of dengue disease is developed using optimal control theory by dividing the population into Susceptible, Exposed, Infected, and Recovered (SEIR) sub-populations. The Pontryagin minimum principle of the fourth-order Runge-Kutta method is used in the model of the spread of dengue disease by incorporating control factors in the form of education and vaccination of susceptible human populations, as well as treatment of infected human populations. Optimum control aims to minimize the infected human population in order to reduce the spread of DHF. Simulations were carried out for two cases, namely when the basic reproduction number R_0 is less than one for disease-free conditions and R_0 greater than one for endemic conditions. Based on numerical simulations of the SEIR epidemic model with controls, it results that the optimal strategy is achieved if education controls, vaccinations, and medication are used.

Introduction

Dengue Hemorrhagic Fever (DHF) is an infection caused by the Dengue Virus (Windawati et al., 2020). There are two living populations that play a role in the spread of DHF, namely humans and mosquitoes that carry the dengue virus (Sabran & Jannah, 2020). Dengue is a viral disease transmitted by Aedes mosquitoes, namely mosquitoes which annually cause infection of nearly 390 million humans (Iin et al., 2020). There are several types that transmit the dengue virus, including Aedes aegypti and Aedes albopictus (Dania, 2016). DHF has symptoms similar to dengue fever, but DHF has additional symptoms such as pain in the pit of the stomach, bleeding in the nose, mouth, and gums, or bruising on the skin (Ministry of Health, 2017).

The spread of DHF can be studied through mathematical modeling. Various mathematical models of DHF have been studied by several researchers, as in (Onyejekwe et al., 2019, Khan & Fatmawati, 2021) Onyejekwe et al by applying optimal control theory. In this study, prevention of DHF was carried out by educating the public and treating it. In this study it is also assumed that

someone who is infected with DHF can transmit the disease if he comes into contact with other individuals. Every individual in the population has the same chance of being infected (Onyejekwe et al., 2019). However, this study did not involve a vaccination control. One method to prevent the spread of DHF is by vaccination (Chamnan et al., 2021). Currently, there is no antiviral treatment for dengue, so future hope for dengue control rests with the development of an effective dengue vaccine. One of the DHF vaccine candidates is the CYD-TDV vaccine which is a recombinant vaccine, namely a vaccine that only uses a portion of the viral DNA and was developed by combining the DNA of other organisms, containing live attenuated tetravalent dengue virus (Dorigatti et al., 2015). Then another study was conducted by Khan et al. In this study, an analysis of the stability of the model for the spread of DHF was carried out in endemic and disease-free conditions (Khan & Fatmawati, 2021).

Optimal control theory was developed to find the optimal way to control dynamic systems (Sethi, 2019). In this study, we will analyze the SEIR (Susceptible-Exposed-Infected-Recovered) epidemic model on the spread of DHF by providing educational controls, vaccinations, and medication to minimize individuals infected with the disease using optimal control theory.

Method

We analyze the optimal control problem in the SEIR-type DFH epidemic model in the following step: first, we determine the SEIR epidemic model on the spread of DHF. Then the equilibrium point will be determined and the model will be linearized using the Jacobian matrix and its stability. The model that has been formed, is developed by adding three control factors, namely education, vaccination, and medication. After that, the objective function will be determined based on the Pontryagin minimum principle. After that, the state and costate equations and their stationary conditions are formed. Furthermore, the model will be simulated with Matlab software with the appropriate parameters to see a comparison of the system without control and with control.

Results and discussion

The model

To construct the DHF model, the population is divided into four sub-populations, namely *Susceptible* $(S(t))$, *Exposed* $(E(t))$, *Infected* $(I(t))$, and *Recovered* $(R(t))$. The total population is $N(t) = S(t) + E(t) + I(t) + R(t)$. The compartment diagram is presented in Figure 1.

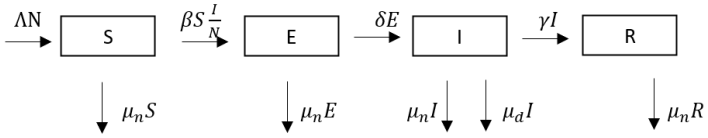

Figure 1. schematic compartment diagram

Based on Figure 1, we have a mathematical model in the form of a system of differential equations as follows.

$$\frac{dS(t)}{dt} = \Lambda N(t) - \beta \frac{I(t)}{N(t)} S(t) - \mu_n S(t)$$
$$\frac{dE(t)}{dt} = \beta \frac{I(t)}{N(t)} S(t) - \mu_n E(t) - \delta E(t) \quad (1)$$

10.12928/bamme.v2i2.7617

$$\frac{dI(t)}{dt} = \delta E(t) - (\mu_n + \mu_d + \gamma)I(t)$$
$$\frac{dR(t)}{dt} = \gamma I(t) - \mu_n R(t).$$

To simplify the model, we normalize the model in Equation (1). In conditions where the total population $N(t)$ is not constant, consider the proportion of each individual compartment in the population,

$$s = \frac{S}{N}, e = \frac{E}{N}, i = \frac{I}{N}, r = \frac{R}{N},$$

where N denotes the total human population. This variable represents the proportion of the total population of each compartment in population N. If these variables are substituted into the model of Equation (1), we get the following equation (See Table 1 for the parameters).

$$\begin{aligned} \frac{ds(t)}{dt} &= \Lambda - \beta is - \mu_n s \\ \frac{de(t)}{dt} &= \beta is - \mu_n e - \delta e \\ \frac{di(t)}{dt} &= \delta e - (\mu_n + \mu_d + \gamma)i \\ \frac{dr(t)}{dt} &= \gamma i - \mu_n r \end{aligned} \quad (2)$$

Table 1. Parameter of the model

Parameter	Meaning
Λ	Recruitmen rate
μ_n	Natural death rate
μ_d	Desease death rate
β	Transmission contact rate
δ	Exposure rate
γ	Recovery rate

The existence of equilibria

The system expressed in Equation (2) have two equilibrium points, i.e. the disease-free equilibrium point $T_1 = \left(\frac{\Lambda}{\mu_n}, 0,0,0\right)$. By applying next generation matrix proccedure we find the basic reproduction number

$$R_0 = \frac{\beta\Lambda\delta}{(\mu_n)(\mu_n + \delta)(\mu_n + \mu_d + \gamma)}.$$

We also have the disease equilibrium point $T_2 = (s^*, e^*, i^*, r^*)$, with $s^* = \frac{\Lambda}{\mu_n R_0}$, $e^* = \frac{\Lambda(R_0-1)}{(\delta+\mu_n)R_0}$, $i^* = \frac{\Lambda\delta(R_0-1)}{(\delta+\mu_n)(\mu_n+\mu_d+\gamma)R_0}$, and $r^* = \frac{\gamma\Lambda\delta(R_0-1)}{\mu_n(\delta+\mu_n)(\mu_n+\mu_d+\gamma)R_0}$.

The equilibrium point T_1 exist if $R_0 < 1$, while the disease equilibrium T_2 will exist if $R_0 > 1$. For stability of equilibrium point. We have the following theorem.

Theorem 1. The disease-free equilibrium point T_1 is locally asymptotically stable if $R_0 < 1$ and unstable if $R_0 > 1$.

Proof.

The Jacobian matrix of system (1) at $T_1\left(\frac{\Lambda}{\mu_n}, 0,0,0\right)$ is

$$J_1 = \begin{bmatrix} -\mu_n & 0 & -\beta\left(\frac{\Lambda}{\mu_n}\right) & 0 \\ 0 & -\mu_n - \delta & \beta\left(\frac{\Lambda}{\mu_n}\right) & 0 \\ 0 & \delta & -\mu_n - \mu_d - \gamma & 0 \\ 0 & 0 & \gamma & -\mu_n \end{bmatrix}$$

which have characteristic polyomial

$$p(\lambda) = (\lambda + \mu_n)(\lambda + \mu_n)[\lambda^2 + (2\mu_n + \mu_d + \gamma + \delta)\lambda + (\mu_n + \delta)(\mu_n + \mu_d + \gamma)(1 - R_0)] = 0 \qquad (3)$$

The roots of Equation (3) are $\lambda_1 = \lambda_2 = -\mu_n$ and the other two roots will have a negative real part if $R_0 < 1$. Hence, T_1 is locally aymptotically stable if $R_0 < 1$ and unstable if $R_0 > 1$. These completes the proof.

Theorem 2. The disease equilibrium point $T_2 = (s^*, e^*, i^*, r^*)$ is locally asymptotically stable if $m_1, m_2, m_3 > 0$ and $m_1 m_2 - m_3 > 0$, where m_1, m_2, m_3 explained in the proof.

Proof.

The Jacobian matrix system (2) at $T_2(s^*, e^*, i^*, r^*)$ is

$$J(T_2) = \begin{vmatrix} \lambda + \frac{\beta\Lambda\delta}{(\delta + \mu_n)(\mu_n + \mu_d + \gamma)} & 0 & \frac{(\delta + \mu_n)(\mu_n + \mu_d + \gamma)}{\delta} & 0 \\ \frac{-\beta\Lambda\delta}{(\delta + \mu_n)(\mu_n + \mu_d + \gamma)} + \mu_n & \lambda + (\mu_n + \delta) & -\frac{(\delta + \mu_n)(\mu_n + \mu_d + \gamma)}{\delta} & 0 \\ 0 & -\delta & \lambda + (\mu_n + \mu_d + \gamma) & 0 \\ 0 & 0 & -\gamma & \lambda + \mu_n \end{vmatrix}$$

which have characteristic equation

$$(\lambda_1 + \mu_n)(\lambda^3 + m_1\lambda^2 + m_2\lambda + m_3) = 0 \qquad (4)$$

where

$$m_1 = (\mu_n + \mu_d + \gamma) + (\mu_n + \delta) + \frac{\beta\Lambda\delta}{(\delta + \mu_n)(\mu_n + \mu_d + \gamma)}$$

$$m_2 = \frac{\beta\Lambda\delta}{(\mu_n + \mu_d + \gamma)} + \frac{\beta\Lambda\delta}{(\delta + \mu_n)}$$

$$m_3 = \beta\Lambda\delta - \mu_n(\delta + \mu_n)(\mu_n + \mu_d + \gamma)$$

Acording to Routh-Hurwitz criteria, all roots of (4) have a negative real part if $m_1, m_2, m_3 > 0$, and $m_1 m_2 - m_3 > 0$. Hence, $T_2(s^*, e^*, i^*, r^*)$ is locally asymptotically stable if $m_1, m_2, m_3 > 0$ and $m_1 m_2 - m_3 > 0$.

Formulation of optimal control problem

In this section we reformulates an optimal control problems of system (2). We use two control functions $u_1(t)$, $u_2(t)$, and $u_3(t)$ which represents the number of susceptible individuals who are given education, vaccination and the number of infected individuals receiving treatment at time t, respectively. The correponding system is

10.12928/bamme.v2i2.7617

$$\begin{aligned}\frac{ds}{dt} &= \Lambda - \beta is - \mu_n s - u_1 s - u_2 s \\ \frac{de}{dt} &= \beta is - \mu_n e - \delta e \\ \frac{di}{dt} &= \delta e - (\mu_n + \mu_d + u_3 + \gamma) i \\ \frac{dr}{dt} &= \gamma i - \mu_n r + u_1 s + u_2 s + u_3 i.\end{aligned} \tag{5}$$

The use of optimal control theory aims to minimize the number of populations infected with the disease so that it is minimum at the end of time t with the following objective function

$$J(u_1, u_2, u_3) = \int_{t_0}^{t_f} \left(A + \frac{1}{2}(B_1 u_1^2 + B_2 u_2^2 + B_3 u_3^2) \right) dt, \tag{6}$$

where A is a balancing factor for costs due to infection and B_1, B_2, and B_3, each of which is the cost of education, vaccination, and treatment with $t \in [0, t_f]$.

Then, we apply the optimal control theory to determine the optimal strategies u and maximizing the objective functional (6) subject to system (5) such that

$$J(\dot{u}_1, \dot{u}_2, \dot{u}_3) = \min J\,(u_1, u_2, u_3) | u_1, u_2, u_3 \in u$$

where

$$u = \{(u_1(t), u_2(t), u_3(t)) : a_p \leq (u_1(t), u_2(t), u_3(t)) \leq b_p, p = 1,2,3\,, t \in [0, t_f]\}$$

The optimal control problem is solved by satisfying the conditions on the Pontryagin minimum principle. We get

$$\begin{aligned}H(x, u, \lambda) = Ai + \frac{1}{2}(B_1 u_1^2 + B_2 u_2^2 + B_3 u_3^2) + \lambda_1(\Lambda - \beta is - \mu_n s - u_1 s - u_2 s) + \lambda_2(\beta is - \mu_n e - \delta e) \\ + \lambda_3(\delta e - (\mu_n + \mu_d + u_3 + \gamma) i) + \lambda_4(\gamma i - \mu_n r + u_1 s + u_2 s + u_3 i)\end{aligned}$$

where $(\lambda_1, \lambda_2, \lambda_3, \lambda_4)$ are costate variables associated with the state variables (s, e, i, r).

Next, according to Pontryagin's minimum principle, the Hamiltonian function reaches an optimal solution if it satisfies the following conditions.

1. Stationer condition for control $u(t)$:

$$\begin{aligned}\frac{\partial H}{\partial u_1} = 0 \quad &\Leftrightarrow \quad B_1 u_1 - \lambda_1 s + \lambda_4 s = 0 \\ &\Leftrightarrow \quad u_1 = \frac{(\lambda_1 - \lambda_4) s}{B_1} \\ \frac{\partial H}{\partial u_2} = 0 \quad &\Leftrightarrow \quad B_2 u_2 - \lambda_1 s + \lambda_4 s = 0 \\ &\Leftrightarrow \quad u_2 = \frac{(\lambda_1 - \lambda_4) s}{B_2} \\ \frac{\partial H}{\partial u_3} = 0 \quad &\Leftrightarrow \quad B_3 u_3 - \lambda_3 i + \lambda_4 i = 0 \\ &\Leftrightarrow \quad u_3 = \frac{(\lambda_3 - \lambda_4) i}{B_3}\end{aligned}$$

Hence, we have

$$u_1 = \begin{cases} 0 & , \text{if } \dfrac{(\lambda_1 - \lambda_4)s}{B_1} < 0 \\ \dfrac{(\lambda_1 - \lambda_4)s}{B_1} & , \text{if } \dfrac{(\lambda_1 - \lambda_4)s}{B_1} = 0 \\ u_{1max} & , \text{if } \dfrac{(\lambda_1 - \lambda_4)s}{B_1} > 0 \end{cases}$$

$$u_2 = \begin{cases} 0 & , \text{if } \dfrac{(\lambda_1 - \lambda_4)s}{B_2} < 0 \\ \dfrac{(\lambda_1 - \lambda_4)s}{B_2} & , \text{if } \dfrac{(\lambda_1 - \lambda_4)s}{B_2} = 0 \\ u_{2max} & , \text{if } \dfrac{(\lambda_1 - \lambda_4)s}{B_2} > 0 \end{cases}$$

$$u_3 = \begin{cases} 0 & , \text{if } \dfrac{(\lambda_3 - \lambda_4)i}{B_3} < 0 \\ \dfrac{(\lambda_3 - \lambda_4)i}{B_3} & , \text{if } \dfrac{(\lambda_3 - \lambda_4)i}{B_3} = 0 \\ u_{3max} & , \text{if } \dfrac{(\lambda_3 - \lambda_4)i}{B_3} > 0, \end{cases}$$

So the optimal control u^* can also characterize by

$$u_1 = \min\left(\max\left(0; \frac{(\lambda_1 - \lambda_4)s}{B_1}\right); u_{1max}\right)$$
$$u_2 = \min\left(\max\left(0; \frac{(\lambda_1 - \lambda_4)s}{B_2}\right); u_{2max}\right)$$
$$u_3 = \min\left(\max\left(0; \frac{(\lambda_3 - \lambda_4)i}{B_3}\right); u_{3max}\right).$$

2. State equations

$$\begin{aligned} \frac{\partial H}{\partial \lambda_1} &= \Lambda - \beta i s - \mu_n s - u_1 s - u_2 s \\ \frac{\partial H}{\partial \lambda_2} &= \beta i s - \mu_n e - \delta e \\ \frac{\partial H}{\partial \lambda_3} &= \delta e - (\mu_n + \mu_d + u_3 + \gamma) i \\ \frac{\partial H}{\partial \lambda_4} &= \gamma i - \mu_n r + u_1 s + u_2 s + u_3 i \end{aligned} \tag{7}$$

3. Costate equation

$$\begin{aligned} \frac{\partial H}{\partial s} &= \lambda_1(\beta i + \mu_n + u_1 + u_2) - \lambda_2 \beta i - \lambda_4(u_1 + u_2) \\ \frac{\partial H}{\partial e} &= \lambda_2(\mu_n + \delta) - \lambda_3 \delta \\ \frac{\partial H}{\partial i} &= -A + \lambda_1 \beta s - \lambda_2 \beta s + \lambda_3(\mu_n + \mu_d + u_3 + \gamma) - \lambda_4(u_3 + \gamma) \\ \frac{\partial H}{\partial r} &= \lambda_4 \mu_n. \end{aligned} \tag{8}$$

Numerical simulations

In this section we gives some numerical simulation to observe the optimal trajectories of the optimal system. We simulate several strategies as follows.

10.12928/bamme.v2i2.7617

Strategy I

Only education as a control strategy, so only u_1 as the control variable. Figure 2 shows the impact of education on the populatin size.

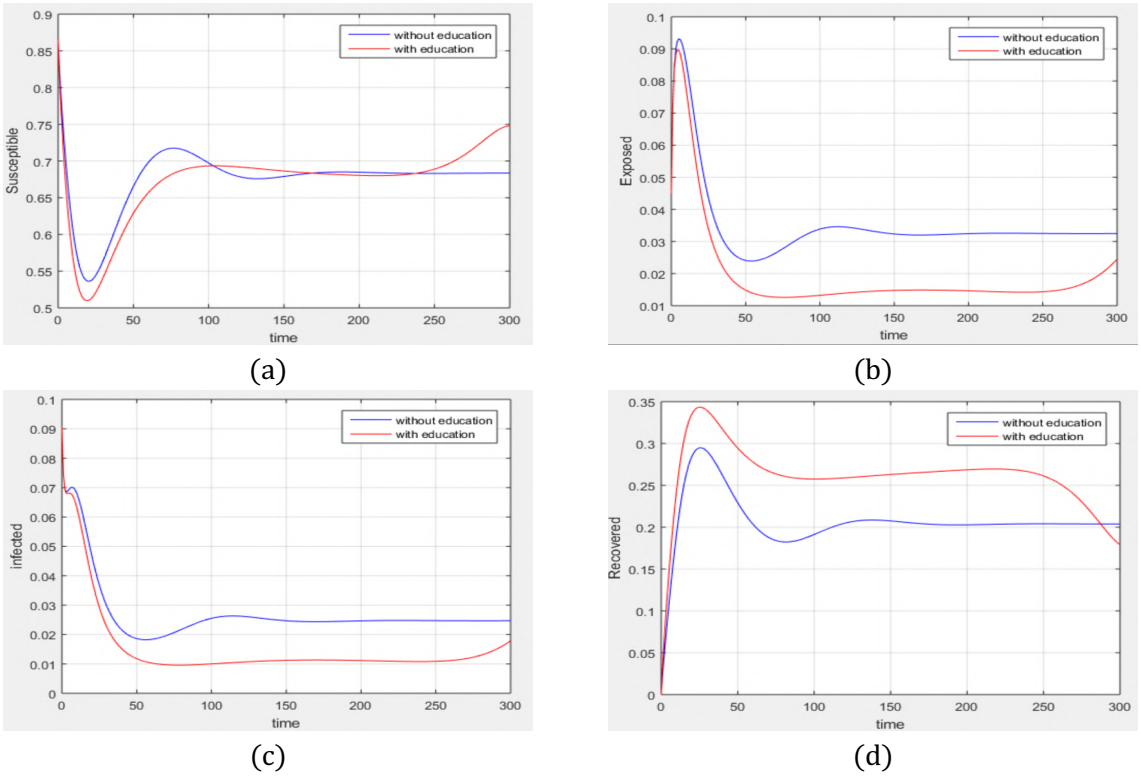

Figure 2. Proportion of the number of susceptible, exposed, infected, and recovered with and without education.

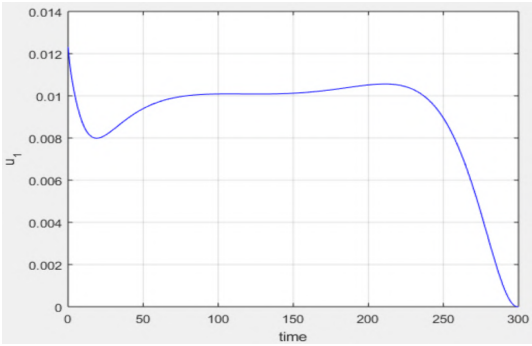

Figure 3. Control profile for Strategy I.

In Figure 2, it can be seen that when there is no control, the susceptible, exposed, infected, and recovered populations are 53.69% respectively; 9.23%; 6.89%; and 18.91%. Then after being given educational controls, the susceptible, exposed, infected, and recovered populations were 69.40%; 1.48%; 1.13%; and 25.39%. Furthermore, the graph of the educational control function can be seen in Figure 3. In Figure 3, from the first day education was given, then on the 250th day the intensity of the education given began to decrease sharply in order to save costs. When the 300th day, education is no longer given. This is possible because when people are given education, people start to become aware of the dangers of DHF.

Strategy II

The control strategy in strategy II is a strategy that considers education and vaccination. The simulation is shown in Figure 4.

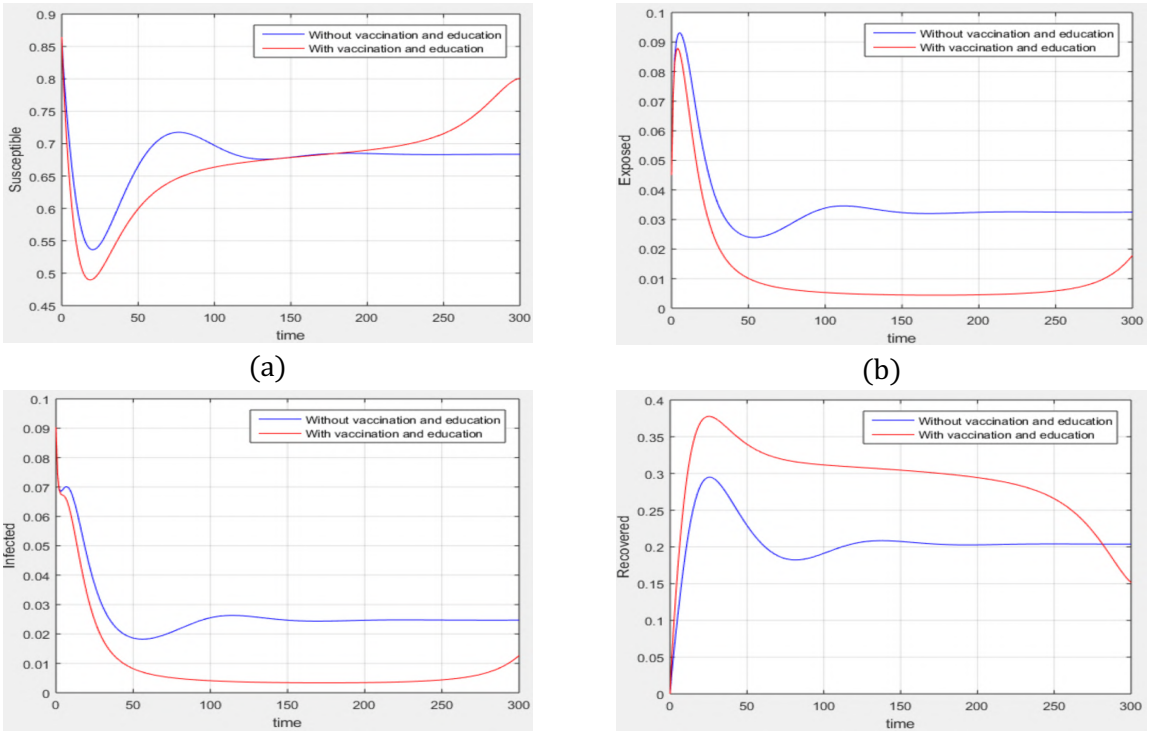

Figure 4. Proportion of the number of susceptible, exposed, infected, and recovered with education & vaccination and without education & vaccination

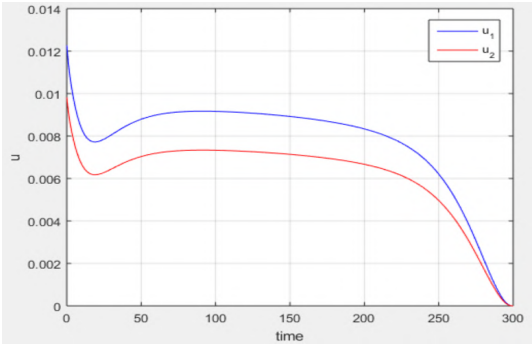

Figure 5. Control profile for Strategy II

In Figure 4, it can be seen that when there is no control, the susceptible, exposed, infected, and recovered populations are 53.69% respectively; 9.23%; 6.89%; and 18.91%. Then after being given educational controls and vaccinations, the susceptible, exposed, infected, and recovered populations were 72.65%; 0.71%; 0.56%; and 28.72%. Furthermore, control profile for Strategy II, the use of education and vaccination control functions can be seen in Figure 5. In Figure 5, the community is given education and vaccination simultaneously. It can be seen that on the 200th day, the provision of education and vaccination began to decrease sharply so as to save costs. This is possible because people are starting to become aware of the dangers of DHF and have strong body immunity.

10.12928/bamme.v2i2.7617

Strategy III

The control strategy in strategy III is a strategy that considers education and treatment. The numerical simulation is shown in Figure 6.

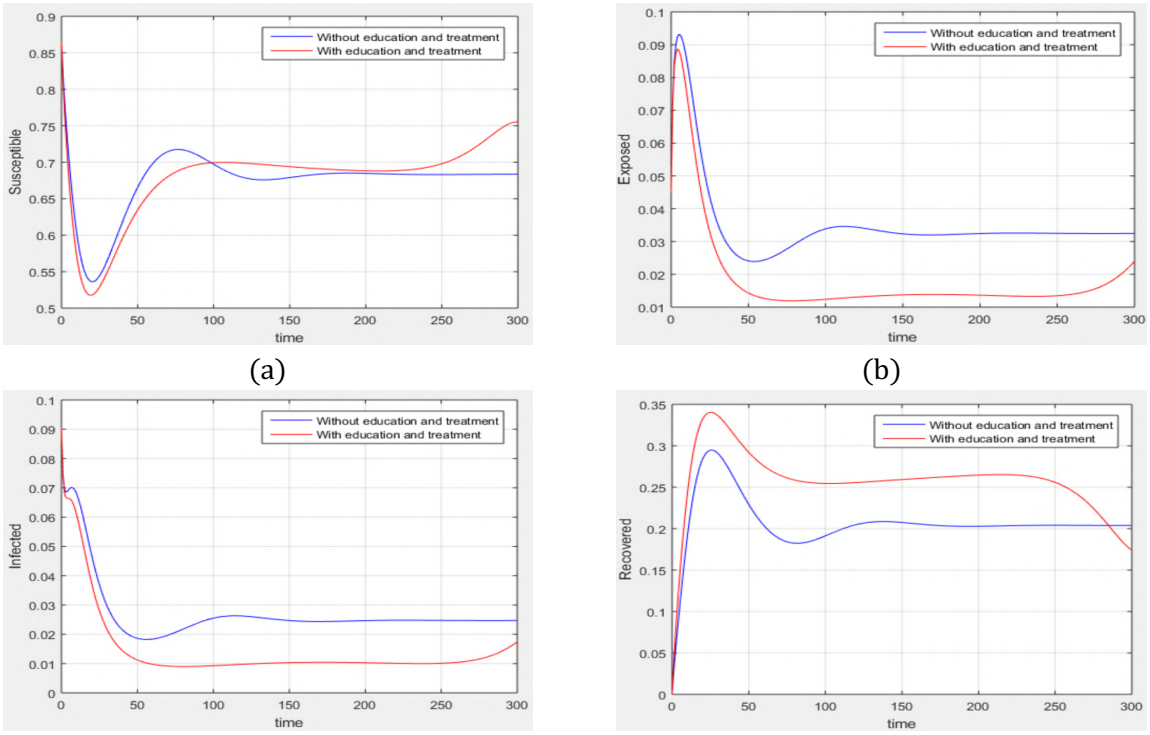

Figure 6. The proportion of the number of susceptible, exposed, infected, and recovered with education & treatment and without education & treatment.

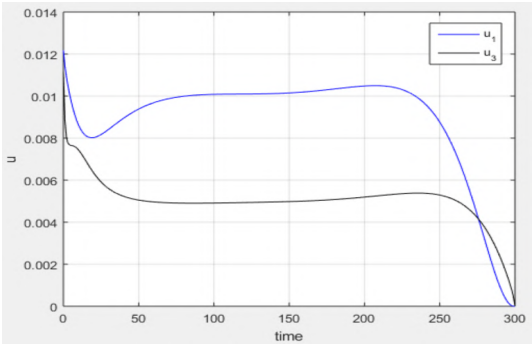

Figure 7. Control profiles for Strategy III.

In Figure 6 it can be seen that when there is no control, the susceptible, exposed, infected, and recovered populations are 53.69% respectively; 9.23%; 6.89%; and 18.91%. Then after being given educational control and vaccination, the susceptible, exposed, infected, and recovered populations were 70.73%; 1.21%; 0.92%; and 26.56%. The graphs of the education and treatment control functions can be seen in Figure 6. In Figure 7 the community is given education and treatment simultaneously. It can be seen that the intensity of providing education and treatment has decreased so as to save costs. This is possible because people are starting to become aware of the dangers of DHF and those infected have recovered.

Strategi IV

The control strategy for strategy IV is a strategy that only considers vaccination. Strategy IV simulation is shown in Figure 8.

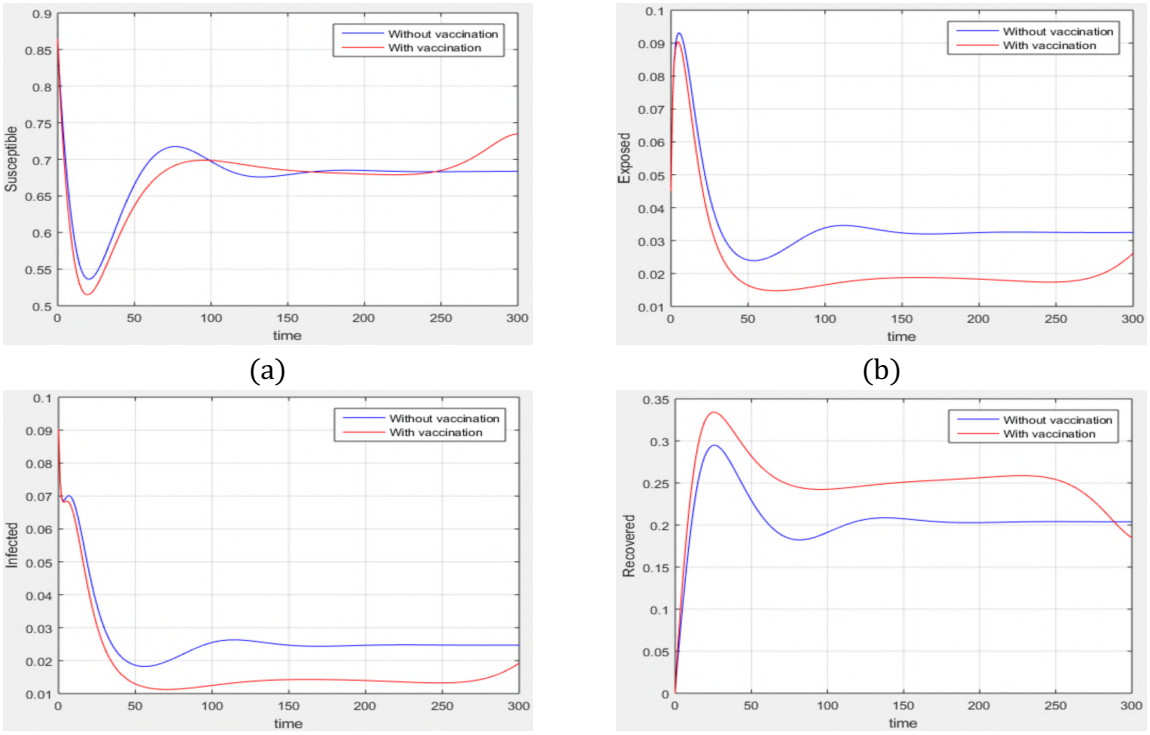

Figure 8. Proportion of the number of susceptible, exposed, infected, and recovered with and without vaccination.

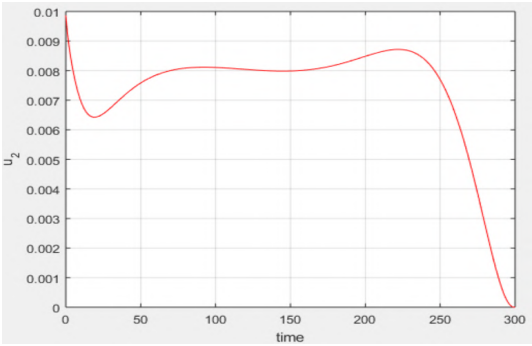

Figure 9. Control profile for Strategy IV.

From Figure 8, we can see that when there is no control, the susceptible, exposed, infected, and recovered populations are 53.69% respectively; 9.23%; 6.89%; and 18.91%. Then after being given educational controls and vaccinations, the susceptible, exposed, infected, and recovered populations were 69.40%; 1.48%; 1.13%; and 25.39%. The graph of the vaccination control function can be seen in Figure 9. In Figure 9 since the first day of vaccination, then on the 250th day the intensity of the vaccination given begins to decrease sharply in order to save costs. On day 300, vaccination is not given. This is possible because when people are vaccinated, people have strong body immunity.

10.12928/bamme.v2i2.7617

Strategi V

Strategy V is a strategy that only considers treatment. The numerical simulation is shown in Figure 10.

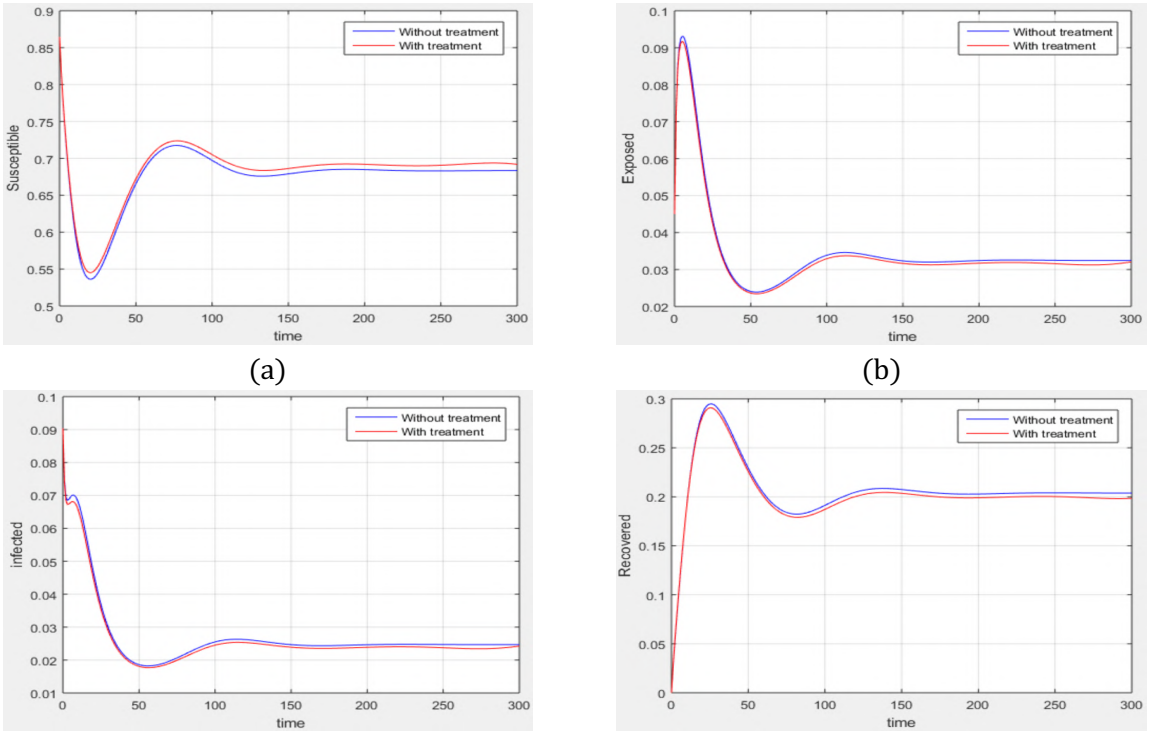

Figure 10. Proportion of the number of susceptible, exposed, infected, and recovered with and without treatment.

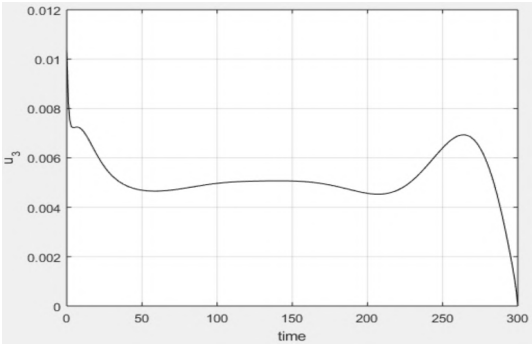

Figure 11 Control profiles for Strategy V.

In Figure 10, it can be seen that when there is no control, the susceptible, exposed, infected, and recovered populations are 53.69% respectively; 9.23%; 6.89%; and 18.91%. Then after being given educational controls and vaccinations, the susceptible, exposed, infected, and recovered populations were 69.09%; 2.55%; 1.88%; and 19.91%. Furthermore, the graph of the treatment control function can be seen in Figure 11. In Figure 11, we can see that on day 280 the intensity of the treatment given began to decrease sharply in order to save costs. When the 300th day, the treatment is no longer given. This is possible because when the infected community is given treatment, the community recovers from DHF.

Strategy VI

The control strategy in strategy VI is a strategy that considers vaccination and medication. The numerical simulation is shown in Figure 12.

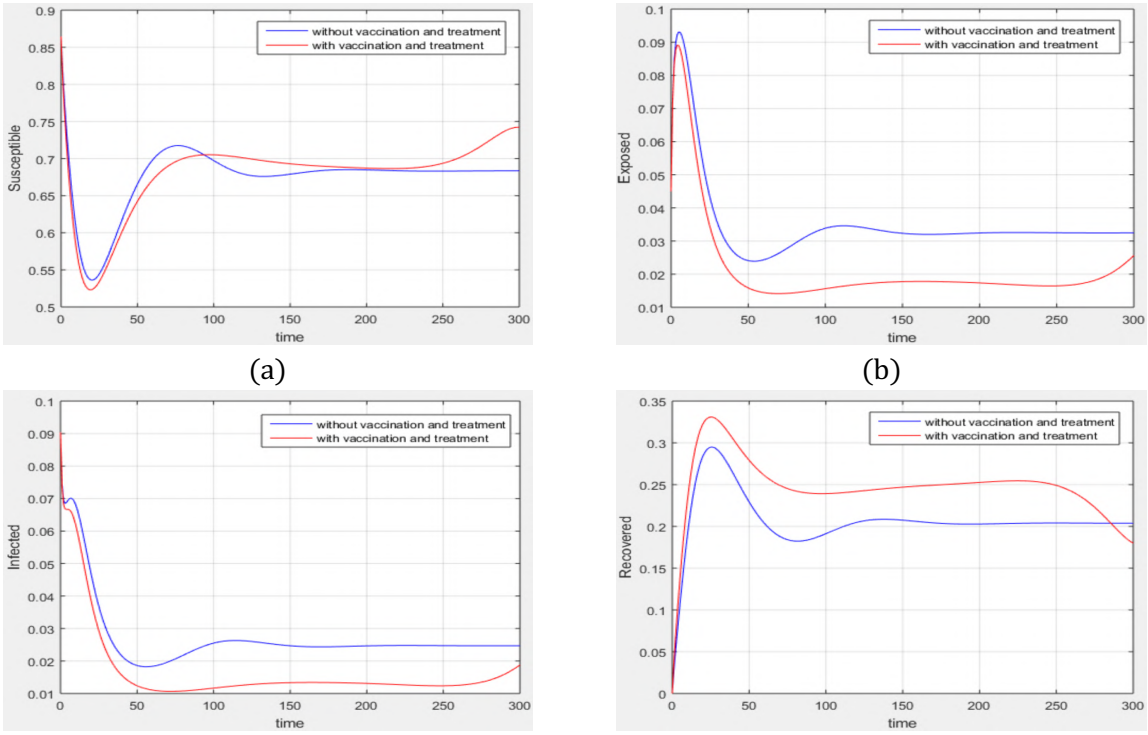

Figure 12. Proportion of the number of susceptible, exposed, infected, and recovered with vaccination & treatment and without vaccination & treatment.

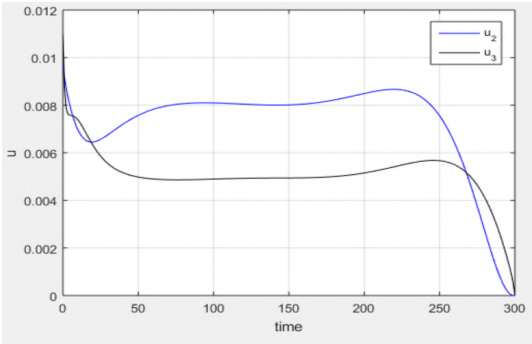

Figure 13. Control profiles for Strategy VI

In Figure 12, it can be seen that when there is no control, the susceptible, exposed, infected, and recovered populations are 53.69% respectively; 9.23%; 6.89%; and 18.91%. Then after being given educational controls and vaccinations, the susceptible, exposed, infected, and recovered populations were 70.22%; 1.41%; 1.07%; and 25%. Then, the graph of the function of vaccination and treatment control can be seen in Figure 13. In Figure 13 the community is given vaccination and treatment simultaneously. It can be seen that the intensity of vaccination and treatment has decreased so as to save costs. This is possible because the community has strong body immunity against DHF and the infected people have recovered.

10.12928/bamme.v2i2.7617

Strategy VII

The control strategy in strategy VII is a strategy that considers education, vaccination, and medication. The numerical simulation is shown in Figure 14.

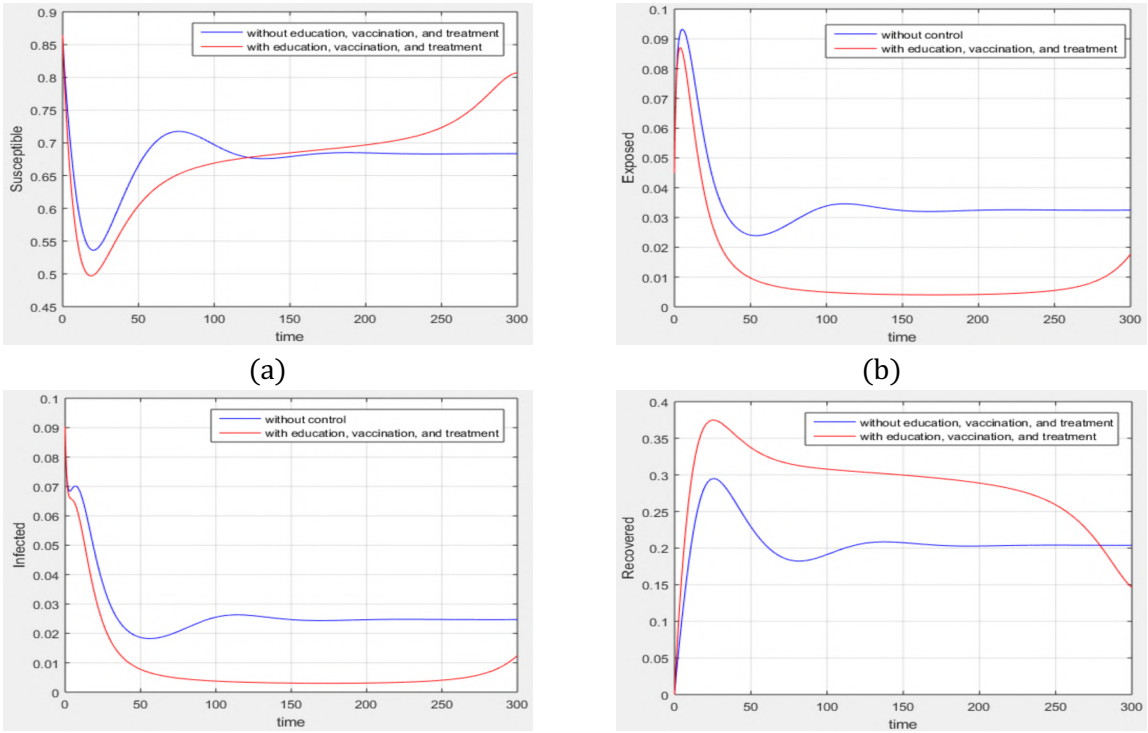

Figure 14. The proportion of the number of susceptible, exposed, infected, and recovered with education, vaccination & treatment and without education, vaccination & treatment.

Figure 14 shows that when there is no control, the susceptible, exposed, infected, and recovered populations are 53.69% respectively; 9.23%; 6.89%; and 18.91%. Then after being given educational controls and vaccinations, the susceptible, exposed, infected, and recovered populations were 73.35%; 0.67%; 0.52%; and 28.20%. Then, the graphs of education, vaccination, and treatment control functions can be seen in Figure 15.

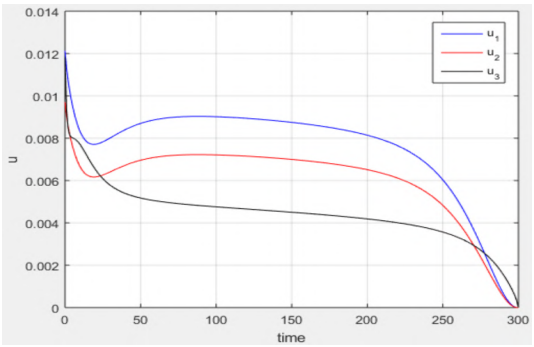

Figure15. Control profile for Strategy VII

Figure 15 shows that the community is given education, vaccination and treatment simultaneously. It can be seen that the provision of education, vaccination, and treatment is decreasing, so it can save costs. This is possible because people are starting to become aware of the

dangers of DHF, have strong body immunity, and people who are infected recover from the disease.

Conclusion

The mathematical model for the spread of DHF used in this paper is the SEIR (Susceptible-Exposed-Infected-Recovered) model. Based on this model, two equilibrium points are obtained, namely T_1 and T_2. Stability analysis was carried out at both of these equilibrium points and it was concluded that the equilibrium points T_1 and T_2 were locally asymptotically stable. The control that has the most influence on the spread of DHF obtained in this paper is educational control. Then, the infected population will decrease more rapidly when educational controls, vaccinations, and medication are used. For the future research, global stability analysis can be carried out on the model. Then, for optimal control of the spread of DHF can be developed using other methods.

References

Chamnan, A., Pongsumpun, P., Tang, I., & Wongvanich, N. (2021). *Local and Global Stability Analysis* of Dengue Disease with Vaccination and Optimal Control. 13, 1–24.

Dania, I. A. (2016). Gambaran Penyakit dan Vektor Demam Berdarah Dengue (DBD). *Majalah Ilmiah* Warta Dharmawangsa, Edisi 48, 1–14.

Dorigatti, I., Aguas, R., Donnelly, C. A., Guy, B., Coudeville, L., Jackson, N., Saville, M., & Ferguson, N. M. (2015). Modelling the immunological response to a tetravalent dengue vaccine from multiple phase-2 trials in Latin America and South East Asia. Vaccine, 33(31), 3746–3751. https://doi.org/10.1016/j.vaccine.2015.05.059

Iin, N. K., Yulianti, D. L., Luron, N. G., Pomalingo, S. F., Noviana, W., & Hidaya, N. (2020). Keterkaitan Antara Kondisi Lingkungan Dan Perilaku Masyarakat Terhadap Keberadaan Vektor Demam Berdarah Dengue (DBD). *Journal of Borneo Holistic Health*, *3*(2), 75–85. https://doi.org/10.35334/borticalth.v3i2.1506

Ministry of Health. (2017). Situasi Penyakit Demam Berdarah di Indonesia Tahun 2017 (pp. 1–7).

Khan, M. A., & Fatmawati. (2021). Dengue infection modeling and its optimal control analysis in East Java, Indonesia. *Heliyon*, *7*, e06023. https://doi.org/10.1016/j.heliyon.2021.e06023

Onyejekwe, O. O., Tigabie, A., Ambachew, B., & Alemu, A. (2019). *Application of Optimal Control to* the *Epidemiology of Dengue Fever Transmission*. *7*, 148–165. https://doi.org/10.4236/jamp.2019.71013

Sabran, L. O., & Jannah, M. (2020). Model Matematika SEIRS-SEI pada Penyebaran Penyakit Demam Berdarah Dengue dengan Pengaruh Suhu. *MAP*, 66–78.

Sethi, S. P. (2019). What Is Optimal Control Theory? *Optimal Control Theory*, 1–26. https://doi.org/10.1007/978-3-319-98237-3_1

Windawati, S., Shodiqin, A., & Aini, A. N. (2020). Analisis Kestabilan Model Matematika Penyebaran Penyakit Demam Berdarah dengan Pengaruh Fogging. 2(1), 1–16.

10.12928/bamme.v2i2.7617